

RESEARCH ON SPATIOTEMPORAL CHARACTERISTICS OF URBAN CROWD GATHERING BASED ON BAIDU HEATMAP

Yunwei MENG¹, Shibao LI², Kang CHEN³, Binbin LI⁴, Ji'en ZHANG⁵, Guangyan QING⁶

^{1, 2, 4, 5} School of Traffic and Transportation, Chongqing Jiaotong University, Chongqing, China

³ School of Civil Engineering, Chongqing Jiaotong University, Chongqing, China

⁶ China Merchants Roadway Information Technology (Chongqing) Co., Ltd, Chongqing, China

Abstract:

With the rapid development of urban transportation and the increase in per capita car ownership, the problem of urban traffic congestion is becoming increasingly prominent. Due to the uneven distribution of crowd in different regions of the city, it is difficult to determine and solve the traffic dynamics congestion. In order to solve the problem that it is difficult to determine the dynamics of traffic congestion areas caused by uneven distribution of vitality in different regions of mountainous cities, a crowded mega mountainous city is selected as research object and it proposes a model to calculate the change characteristics of regional crowd gathering. Baidu Heatmap is used as it could distinguish crowd gathering in certain urban core area. The heat map pictures in dozens of consecutive days is extracted and researchers conducted pixel statistical classification on thermal map images. Based on the pixel data of different levels of the pictures, the calculation model is established and an algorithm based on particle swarm optimization is proposed. The calibration of the relative active population equivalent density is conducted, and the distribution characteristics of crowd gathering in time and space are analyzed. The results show that there are obvious spatiotemporal characteristics for this selected city. In time, holidays have an important impact on crowd gathering. The peak time of crowd gathering on weekdays is different from that on rest days. The research in this paper has a direct practical value for the identification of traffic congestion areas and the corresponding governance measures. The dynamic identification of population gathering areas in mountainous mega cities, demand prediction for various transportation regions, and future population OD(Origin—Destination) planning are of great significance.

Keywords: Crowd Gathering, Baidu Heatmap, Urban Core Area, Spatiotemporal Characteristics, Population Equivalent Density

To cite this article:

Meng, Y., Li, S., Chen, K., Li, B., Zhang, J., Qing, G., (2023). Research on spatiotemporal characteristics of urban crowd gathering based on Baidu heatmap. Archives of Transport, 68(4), 41-54. DOI: <https://doi.org/10.61089/aot2023.1g53c194>



Contact:

1) 514346081@qq.com [<http://orcid.org/0000-0001-8605-4920>] – corresponding author; 2) 571187537@qq.com [<http://orcid.org/0009-0008-3078-9205>]; 3) 2606011182@qq.com [<http://orcid.org/0009-0001-3625-5086>]; 4) 1506764862@qq.com [<http://orcid.org/0000-0003-2493-5129>]; 5) 1140840698@qq.com [<http://orcid.org/0009-0008-8053-2256>]; 6) 379544277@qq.com [<http://orcid.org/0009-0009-9364-2662>]

1. Introduction

In mountainous mega cities, the terrain conditions are special, and the road alignment is complex and changeable. The terrain determines the direction, layout and scale of the road. The completion of the road network has promoted the development of transportation. The increase of vehicle ownership worsens the traffic congestion, resulting in increasingly serious traffic congestion problems. The current measures to deal with traffic congestion are often very passive and inefficient. To solve the problem of traffic congestion, it is necessary to study the gathering and spatial distribution of the crowds.

Baidu Heatmap can identify the crowd gathering situation in the urban core area, and it can identify dynamic crowd gathering areas in real time, which is conducive to taking flexible response measures. Therefore, the recognition research of using Baidu Heatmap has attracted high attention from relevant researchers all over the world.

The purpose of this paper is to use the crowd gathering data collected by Baidu Heatmap to analyze the changes of crowd move activities between different traffic districts in the urban core area of Chongqing, explore the rules of crowd gathering, and make contributions to transportation planning.

2. Literature review

The number of roads in the network determines the traffic carrying capacity (Liu SQ. 2022). With the rapid development of geographic information technology, the application of big data enables researchers to dynamically study the spatiotemporal behavior of people from a more precise scale, providing new ideas for urban planning and management. At present, big data such as the heat maps can fill the data gap in urban vitality research to a certain extent. Its principle is to obtain the location information of mobile terminals through radio communication networks or external positioning, and then describe the crowd gathering in real time by superimposing color blocks on the map (Chen W. 2020).

With the dynamic, real-time, massive, fast, diverse and other characteristics of big data such as Baidu Heatmap, its geographic information data has attracted more and more scholars' attention and research (An M, et al. 2014). As a big data application based on the geographic and spatial location of hundreds of millions of mobile phone users, Baidu Heatmap provides a large amount of data support to

study the characteristics of urban crowd gathering. Chen Y and Yang J employed big data and pedestrian simulation technologies to diagnose facility shortages and traffic problems in the area(Chen Y et al.2020). Nieroda et al. thinks that heatmaps are a method for efficiently collecting large amounts of data. And the efficiency of traffic sign recognition was evaluated by collecting data using this heatmap (Nieroda et al.2022). Moreover, the heatmap can be used to evaluate the efficiency of the analysis model. Chen Z proposed a short-term traffic flow prediction framework and a heatmap was produced to visualize the predicted speed(Chen Z et al.2021).

To solve traffic congestion in mega mountain cities, research has been conducted in many areas of transportation with the help of heat maps. Kozłowska A et al. proposed a method for predicting urban population travel activities based on social media data(Kozłowska A et al.2020). Chen S et al. analyzed the differences between mountain cities and plain cities and improved the definition of road network density and connectivity (Chen S. 2018).Chen Y et al. analyzed the impact of traffic management policies on traffic evacuation in catastrophic disaster situations and constructed a traffic simulation model that to support the improvement of traffic management policies (Chen Y,et al.2020).Du X et al. considered heat map as an intuitive and accurate tool for visualizing spatial data, and it conducted a heat map test of traffic development index based on geographic information data of some countries to verify the feasibility and reliability of heat map for traffic state identification (Du X,et al. 2022).Khan et al. obtained traffic data through a network and proposed a method to establish communication between vehicles in real time (Khan M and Arora B. 2021) . Liu YS et al. analyzed the spatiotemporal characteristics of urban vitality and related influencing factors in the sixth ring area of Beijing based on heat map and interest point data (Liu Y S, et al. 2018) Lu Y et al. analyzed the problems in current traffic planning by combining network traffic data with the help of user equilibrium model (Lu Y. 2020). Based on the data from Baidu Heatmap, Tan X et al. compared and analyzed the job-dwelling relationship and spatial characteristics of the Chongqing main urban areas (Tan X, et al. 2016). Tang KZ et al. proposed an improved particle swarm optimization algorithm based on the standard particle swarm optimization algorithm to improve the computational efficiency Tang

K Z, et al. 2015). Valencia et al. used the VISSIM program to propose a theory for reducing traffic congestion and conflicts, improving traffic conditions, and adjusting traffic operation patterns (Valencia A, et al.2020). Taking the main urban area of Wuhan city as an example, Wang CL analyzed the fluctuation characteristics of the crowd gathering on weekdays and rest days, and it found that the volatility of weekdays is stronger than that of rest days, there is a phase difference in travel time, and the travel time range is longer in rest days (Wang L C. 2018).Wei et al. proposed a new urban traffic planning model under spatiotemporal constraints of crowded gathering, and then some treatment countermeasures were provided for traffic planning and management (Wei, L.Y, et al. 2021). Wu et al. analyzed the spatiotemporal variation of heat intensity distribution and the change of population gravity center in Shanghai based on the dynamic big data of Baidu Heatmap (Wu Z Q, et al. 2016). Yu C et al. studied the spatiotemporal characteristics of urban public transportation travel demand using heat map data (Wang Z C, et al. 2013). Yang J et al. studied the population flow characteristics using data from Baidu maps, and it used a commuter trip identification method based on travel chain analysis to screen commuter flows and analyze the regional changes in population flows by combining the passenger flows in and out of subway stations in the morning and evening peaks (Yang J, et al. 2021). With the help of heat map data, Zhou Y F et al. conducted a study to measure the vitality of the service area of Shenzhen metro rail transit stations (Zhou Y F, et al. 2020).Wang Z C et al. proposed an interactive urban traffic congestion visualization and system based on GPS trajectories, and it developed a strategy to extract traffic congestion information and draw a heat map of traffic conditions to make traffic information more intuitive (Wang Z C, et al. 2013).

Many scholars around the world have conducted research on urban spatial structure and crowd gathering characteristics, but it is not difficult to find that there is a lack of research on population density and travel patterns combined with heat maps. This paper takes the urban core area of Chongqing, P.R.C as the research object, and then map heat map is extracted and analyzed to explore the hotspot areas of different urban areas. A method for calculating the aggregation state of a crowd gathering is proposed. The spatiotemporal characteristics and differences of travel

activities between different traffic districts are analyzed.

3. Data overview and pre-processing

3.1. Data sources

Baidu Heatmap is a big data visualization product launched by Baidu Map, which is based on the geographic location data of cell phone users on the mobile location service platform. Through the geographic location information sent by users when they visit, a series of algorithms analyze and process the data to calculate the speed of people flow and population density in various areas within the city, and finally present users with different levels of crowd gathering, i.e., by overlaying different color blocks on the map. Users of the map product generate a huge volume of geographic information data, so it is of great value and significance to apply the data of heat map to various professional fields through statistics and analysis.

The main urban area of Chongqing consists of 9 urban districts: Yuzhong, Jiangbei, Nan'an, Jiulongpo, Shapingba, Dadukou, Beibei, Yubei and Banan. The resident population of main urban area is about 20,329,000, and the core urban areas of Chongqing are Shapingba, Nan'an, Yuzhong and Yubei. These 4 districts contain relevant streets with developed traffic and economy, and contain tourist attractions, the average number of active vehicles per day in the inner ring on weekdays is over 400,000. The daily crowd gathering is huge (Huang Y, et al. 2019).

The topography of Chongqing is special, showing "two rivers and four hills", which leads to a small area of land available for urban construction. The core urban area is developed with high intensity and the population density is highly concentrated with a large traffic flow for commuting during the morning and evening peak. The traffic demand in the core area is much higher than the traffic supply, which contributes to the regular traffic congestion (Huang Y, et al. 2019). As shown in Fig. 1 and Fig. 2, according to the urban land function, the city is divided into residential land, public management service facility land, commercial service facility land, industrial construction site, logistics storage land, road and transportation facility land, public facility land, green land and square land. Based on the land function, the core area is divided into 111 traffic districts, numbered 1, 2, 3, in order. Using the map of urban land function, the data of land use relating to

crowd gathering are extracted from each traffic district.

The heat maps are obtained for a total of 76 days from September 1, 2020 to November 18, 2020 (with data missing for September 22, October 25 and 26) within the core area of the city by registering and

logging into the API interface in the map open platform. The heat maps are sampled on a daily basis from 07:00 a.m. to 21:00 p.m. each day, and it is acquired at 10-minute intervals. So a total of 6,739 heat maps is obtained. A typical heat map is shown in Fig. 3.

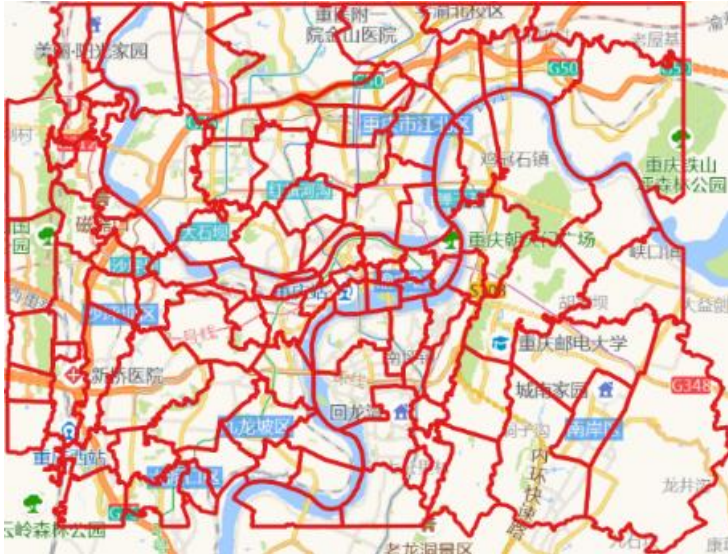


Fig. 1. Traffic district



Fig. 2. Land function of urban area

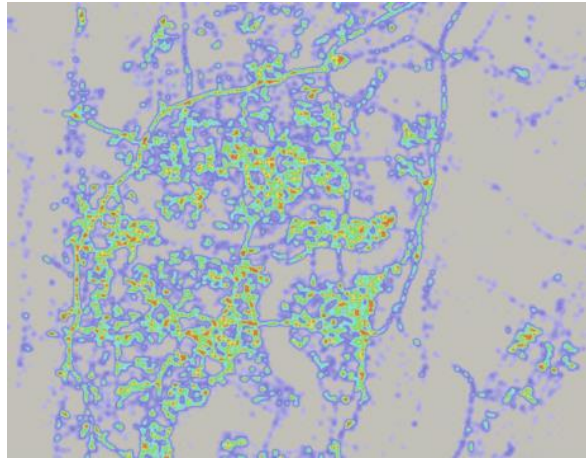


Fig. 3. Heat map of Chongqing at 12:00 on 5th, November

3.2. Data Extraction

The heat map is a raster picture in PNG format, and each heat map contains 15360×11880 pixel points. In order to be able to extract each pixel point accurately, the pixels in the heat map are divided into 10 categories. These 10 categories correspond to 10 colors, namely red, orange, yellow, green, cyan, cyan-violet, violet, light violet, purple-gary and gray. Their corresponding RGB functions in the color gamut are shown in Table 1.

As shown in Fig. 4, the pixel points in the obtained 6739 heat maps are identified and extracted by applying MATLAB software according to the 10 categories above, and the data extraction has been done. From the extracted color, it is still impossible to distinguish the gathering state of the crowd. Therefore,

it is necessary to further calculate the 10 categories of colors to determine the quantitative relationship between different colors and crowd gathering.

Table 1. Pixel color gamut value

Category	Color	RGB(Red,Green,Blue)
1	Red	RGB(160:255,0:100,0:90)
2	Orange	RGB(160:255,101:255,0:90)
3	Yellow	RGB(180:255,101:255,91:140)
4	Green	RGB(110:179,195:255,85:195)
5	Cyan	RGB(120:170,200:235,196:255)
6	Cyan-violet	RGB(120:160,165:199,200:255)
7	Violet	RGB(100:160,110:164,190:255)
8	Light violet	RGB(161:185,151:165,200:255)
9	Purple-gary	RGB(161:200,166:199,200:255)
10	Gray	RGB(181:255,181:255,181:199)

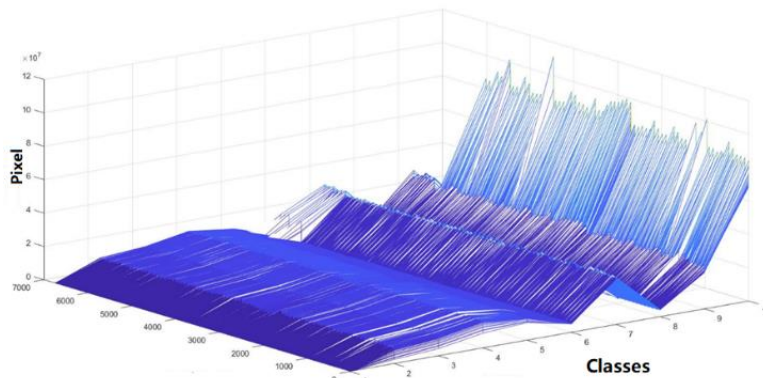


Fig. 4. Pixel statistical distribution

4. Model construction and solution

4.1. Model Construction

The least squares method is a numerical optimization method that solves the best-fitting function of the system by minimizing the square of the error. By establishing an equilibrium relationship between the errors, it can well prevent the extreme effects brought by special conditions and better apply to reveal the state of the system closest to the real condition. In this paper, it needs to find out the closest color category deriving from the heat map data in order to facilitate the classification of crowd gathering for each neighborhood. The least squares optimization application in multiple linear regression is used in model construction.

Taking the category 10 gray as the base color, the active population density represented by unit pigment points of classes 1 to 9 is assumed to be X, as shown in Eq. (1).

$$X = \begin{bmatrix} x_1 \\ x_2 \\ \vdots \\ x_9 \end{bmatrix} \tag{1}$$

A_{ijk} represents the number of k-type pixels in the j^{th} cell corresponding to the i-th hour. The set of 9 categories of pixel points corresponding to the 10 measured traffic districts at the k^{th} hourly moment is known to be $A_{i,j,k}$. Then

$$A_{i,j,k} = \begin{bmatrix} A_{1,1,k} & A_{1,2,k} & \cdots & A_{1,9,k} \\ a_{1,1,k} & a_{1,2,k} & \cdots & a_{1,9,k} \\ a_{2,1,k} & a_{2,2,k} & \cdots & a_{2,9,k} \\ \vdots & \vdots & \ddots & \vdots \\ a_{10,1,k} & a_{10,2,k} & \cdots & a_{10,9,k} \end{bmatrix} \tag{2}$$

where: $a_{i,j,k}$ represents the number of pixel points of the j^{th} category for the i^{th} traffic district corresponding to the k^{th} hourly moment.

It is known that the population number of the k^{th} hour moment corresponding to the 10th measured traffic district is \hat{Y} , as shown in Eq. (3).

$$\hat{Y} = \begin{bmatrix} y_{1,k} \\ y_{2,k} \\ \vdots \\ y_{10,k} \end{bmatrix} \tag{3}$$

According to the least squares model, the condition that should be satisfied here is

$$Y = a_1x_1 + a_2x_2 + \cdots + a_9x_9 \tag{4}$$

The objective function of Eq. (4) is

$$\begin{aligned} \min z = & \sum_{k=1}^{11} \left(\begin{bmatrix} a_{1,1,k} & a_{1,2,k} & \cdots & a_{1,9,k} \\ a_{2,1,k} & a_{2,2,k} & & a_{2,9,k} \\ \vdots & & \ddots & \vdots \\ a_{10,1,k} & a_{10,2,k} & \cdots & a_{10,9,k} \end{bmatrix} \cdot \begin{bmatrix} x_1 \\ x_2 \\ \vdots \\ x_9 \end{bmatrix} - \begin{bmatrix} y_{1,k} \\ y_{2,k} \\ \vdots \\ y_{10,k} \end{bmatrix} \right)^2 \\ = & \sum_{k=1}^{11} (A_{i,j,k} \cdot X - \hat{Y}) \end{aligned} \tag{5}$$

The constraint should satisfy

$$\begin{bmatrix} 0 & 0 & 0 & 0 & 0 & 0 & 0 & 0 & -1 \\ 0 & 0 & 0 & 0 & 0 & 0 & 0 & -1 & 1 \\ 0 & 0 & 0 & 0 & 0 & 0 & -1 & 1 & 0 \\ 0 & 0 & 0 & 0 & 0 & -1 & 1 & 0 & 0 \\ 0 & 0 & 0 & 0 & -1 & 1 & 0 & 0 & 0 \\ 0 & 0 & 0 & -1 & 1 & 0 & 0 & 0 & 0 \\ 0 & 0 & -1 & 1 & 0 & 0 & 0 & 0 & 0 \\ 0 & -1 & 1 & 0 & 0 & 0 & 0 & 0 & 0 \\ -1 & 1 & 0 & 0 & 0 & 0 & 0 & 0 & 0 \end{bmatrix} \cdot \begin{bmatrix} x_1 \\ x_2 \\ x_3 \\ x_4 \\ x_5 \\ x_6 \\ x_7 \\ x_8 \\ x_9 \end{bmatrix} < \begin{bmatrix} 0 \\ 0 \\ 0 \\ 0 \\ 0 \\ 0 \\ 0 \\ 0 \\ 0 \end{bmatrix} \tag{6}$$

Therefore, the model is established. Next, we will solve the model and determine whether there is a solution.

4.2. Model Solution

The goal of the particle swarm optimization algorithm is to make all particles find the optimal solution in a multidimensional space. Each particle contains a position vector and a velocity vector in the multidimensional space, and each particle saves its searched optimal position as it searches in the multidimensional space. At the beginning of each iteration, the particle adjusts its velocity vector and position vector according to its designed parameters and the optimal positions saved by other particles, until it obtains the global optimal position in the whole search space.

In this study, the relative active population equivalent density of different pixel categories within the calibrated density range can be treated as a particle. Therefore, the value of calibration density can be regarded as particle swarm.

It is assumed here that a particle swarm consists of the equivalent active population density corresponding to M pixels of different categories. Each particle needs to find its optimal position in an N -dimensional space. Then, the equivalent population density corresponding to each pixel of different categories is assigned a position, which is represented by X_i .

$$X_i = (x_i^1, x_i^2, \dots, x_i^N), i = 1, 2, 3, \dots, M \quad (7)$$

Its adaptation value is calculated by bringing x_i into the objective function, and the current position x_i is judged to be optimal according to the adaptation value. In each search process, the optimal position P_i for each population equivalent of different categories unit pixel points will be recorded.

$$P_i = (p_i^1, p_i^2, \dots, p_i^N), i = 1, 2, 3, \dots, M \quad (8)$$

The optimal solution of the optimal location of the active population equivalent for all different categories for unit pixel points in this search process can be taken as the optimal search location for the entire calibrated density, which is represented by G_i .

$$G_i = (g_i^1, g_i^2, \dots, g_i^N), i = 1, 2, 3, \dots, M \quad (9)$$

The updating method of velocity vector and position vector of population equivalent of different categories of unit pixels is as follows:

$$v_i^d = wv_i^d + c_1r_1(p_i^d - x_i^d) + c_2r_2(p_g^d - x_i^d) \quad (10)$$

$$x_i^d = x_i^d + \alpha v_i^d$$

Where: $i = 1, 2, \dots, M$, $d = 1, 2, \dots, N$; w is a non-negative number called inertia factor, which determines the convergence of the particle swarm optimization algorithm; P_i is the local optimum position and P_g is the global optimum position; c_1, c_2 is a non-negative constant called acceleration constant, which is used to adjust the coefficients of the weights of the local optimum and the global optimum; r_1, r_2 is a random number in the range of $[0,1]$;

α is the constraint factor, which is used to limit the weight of the velocity.

The optimal solution can be finally obtained by programming the above model through MATLAB, from which the equivalent density X (thousands) of active population represented by 1~9 categories of unit pixels can be obtained, as shown in Table 2 below. The model convergence process is shown in Fig. 5, which shows that the model calculation results can converge, indicating that the model has solutions.

Table. 2. Representative values of population corresponding to pigment categories

Color	Red	Orange	Yellow	Green	Cyan
Density	3.5405	3.5399	3.5395	0.0934	0.0025
Color	Cyan-violet	Violet	Light violet	Purple gray	Gray
Density	0.0015	0.0012	0.0006	0.0004	0

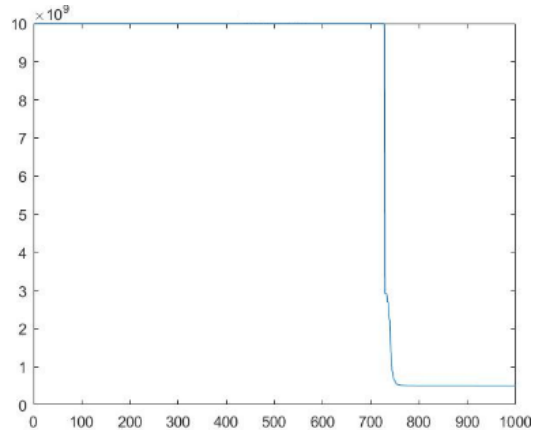


Fig. 5. Convergence process of the algorithm

5. Spatiotemporal Characteristics of Urban Crowd Gathering

5.1. Temporal characteristics of crowd gathering

5.1.1. The overall change pattern of crowd gathering

The overall change of crowd gathering is shown in Fig. 6. The horizontal axis indicates the moments in the study period, and the vertical axis indicates the relative active population equivalents. The different colored dashes indicate the change pattern of different numbered traffic districts. The calculation of the active population equivalent matrix is shown in Eq. (11).

$$H_{6739 \times 111} = \begin{bmatrix} (A_{1,111 \times 10} \cdot X)^T \\ (A_{2,111 \times 10} \cdot X)^T \\ \vdots \\ (A_{6739,111 \times 10} \cdot X)^T \end{bmatrix}_{6739 \times 111} \quad (11)$$

Where, $H_{6739 \times 111}$ is the matrix of relative active population equivalents for 111 districts at 6739 statistical moments; $A_{i,111 \times 10}$ is the matrix of 10 different categories of pixel points for 111 districts at the i th moment; X is the equivalent number of relative active population corresponding to the unit pixel of different pigments categories.

From Fig. 6, it can be found that there is a clear correlation between crowd gathering characteristics and different numbered districts and major holidays. Different numbered districts show different degrees of crowd gathering. Although differences in the number of population equivalents occur between various districts, they always fluctuate around a fixed number of relative active population equivalents. At the same time, a large "gap" in the relative active population equivalents can be observed around the 3000th hour. This position coincides with the timing of the Chinese National Day. The time period represented by the "gap" starts at 7:03 p.m. on October 1 (the 2609th moment) and ends at 21:53 p.m. on October 8 (the 3328th moment), which shows that the National Day has an important impact on population activity.

5.1.2. Daily variation of crowd gathering

The study period of the daily variation of crowd gathering is from 07:03 to 21:53 every day, with an interval of 10 minutes, containing a total of 90 moments of crowd gathering status. After the calculation process, the daily average variation pattern shown in Fig. 7 is presented. The horizontal axis represents the 90 moments from 07:03 to 21:53 each day, and the vertical axis represents the daily relative active population equivalents, and the dash line reflects the daily average variation pattern of the whole day. The relative population equivalents are shown in Eq.(12).

$$H_d = \sum_{i=1}^{111} D_{90 \times 10} \cdot X \quad (12)$$

where H_d is the relative active population equivalent for 90 moments in a day; $\sum_{i=1}^{111} D_{90 \times 10}$ is the

sum of the pixel points of 111 districts containing 10 different pigments categories for 90 moments in a day; and X is the relative active population equivalent per pixel point.

From Fig. 7, it can be seen that the degree of resident's crowd gathering in a day is significantly related to their daily resting time. The minimum and the maximum values of the crowd gathering occur within the selected study period. The minimum value is at 07:03 in the morning, indicating a lower population density at that time, and the maximum value is at 18:33 in the afternoon, indicating a higher population density at that time. During the period from 07:03 a.m. to 09:33 a.m., the crowd gathering in the urban area increases significantly; in the subsequent hours, the gathering remains above and below the value of 70,000 relative population density. At 12:03 p.m., the gathering in the urban area reaches a maximum value. At 14:33 p.m., the crowd gathering reaches another maximum value. In the afternoon, the crowd gathering increased slowly from 16:13 to 18:33. After 18:33, the crowd gathering decreased gradually, indicating that the late peak of the crowd gathering is in the two hours before and after 18:33. The crowd gathering in the afternoon is stronger than that in the morning, and the crowd gathering in a day reaches the peak around 18:33 p.m.

5.1.3. Comparison of crowd gathering characteristics between weekdays and rest days

The relative active population densities of weekdays (excluding weekends and Chinese national holidays) and rest days (including weekends and Chinese national holidays) are calculated separately. After calculation and processing, the characteristics shown in Fig. 8 are presented. The horizontal axis represents the 90 moments of the day on weekdays and rest days, and the vertical axis represents the number of relative active population equivalents. The blue dash represents the relative active population equivalents on weekdays and the red dash represents those on rest days.

In Fig. 8, a clear correlation can be found between the crowd gathering in weekdays and the work days of residents. The relative active population equivalents on weekdays gradually increase from 7:03 a.m. to 9:03 a.m., and then the relative active population equivalents in the whole urban area remain at about 70,000 for 7-8 hours. Around 16:33 p.m., the relative active population equivalents start to increase.

The relative active population equivalents in the urban area start to increase around 16:33 p.m. and reach a peak density of about 80,000 at around 18:33 p.m. Then it gradually decreases until the end of the study period. It also is found that the relative

activity population density in the afternoon of the weekday is generally greater than that in the morning, and the peak relative activity population equivalent of the weekday occurred at around 18:33 p.m.

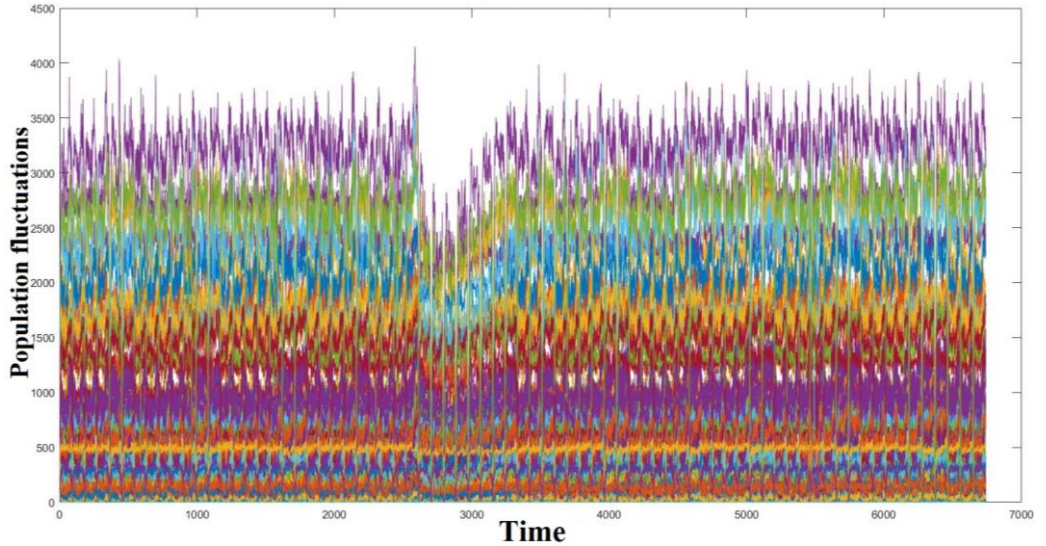


Fig. 6. Overall change in relative population equivalent

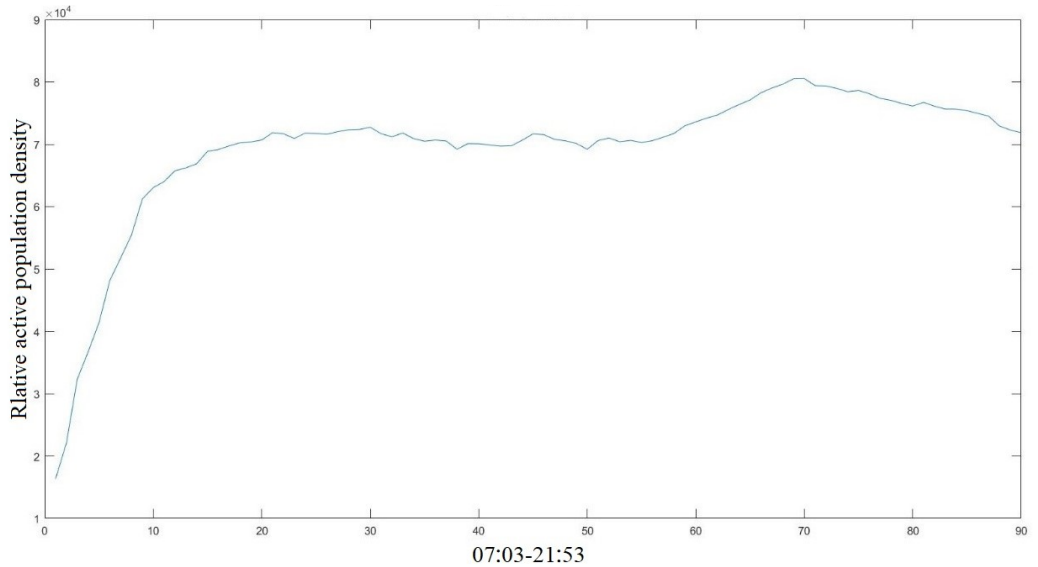


Fig. 7. Daily average variation

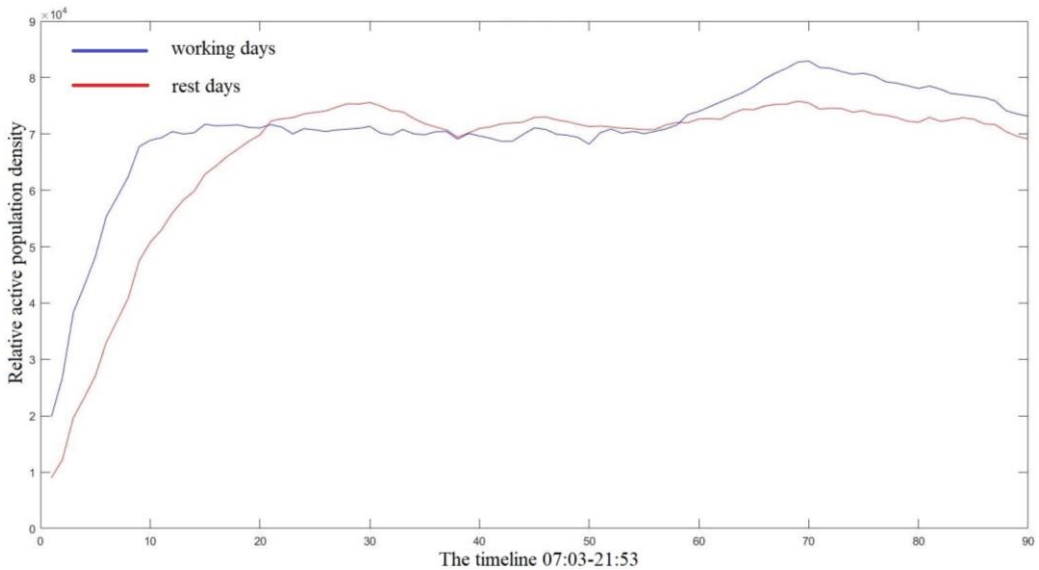


Fig. 8. A comparison of changes between working days and rest days

In Fig. 8, it can be found that the crowd gathering on rest days are significantly correlated with residents' rest trips. The relative active population density on rest days gradually increases from 7:03 a.m. to 10:33 a.m.; at around 12:03 p.m., the relative active population equivalent reaches the peak equivalent of 75,000. Then the relative active population equivalent slowly decreases until around 13:23 p.m. For the other of the rest days, the relative active population equivalent in the urban area fluctuates back and forth around 70,000, indicating that the active population remains stable during this period. It is also found that the relative active population equivalents at noon on the rest day are higher in the day, and the peak of the relative active population equivalents on the rest day occurs at around 12:03 pm.

In Fig. 8, differences in population equivalents between weekdays and rest days can be observed. The relative active population equivalents on weekdays fluctuate around 09:03, while the relative population equivalents on rest days fluctuate around 10:33. The peak relative active population equivalent on weekdays occurs around 18:33 p.m., while the peak relative active population equivalent on rest days occurs around 12:03 p.m. The relative active population equivalents in the afternoon on working days are larger than those in the morning, while the relative

active population equivalents at noon on rest days are larger than those at any other time of the day.

5.2. Spatial Characteristics of Crowd Gathering

The crowd gathering degree of 111 different numbered traffic districts is calculated. The degree of crowd gathering is presented as shown in Fig. 9. The horizontal axis indicates the numbered traffic districts, and the vertical axis indicates the relative active population equivalent. The different color dashes indicate the change of relative active population equivalents.

From Fig. 9, it can be seen that since the relative active population equivalents of each numbered traffic district change continuously, the change of the fold line can reflect the degree of crowd gathering. It can be judged that the numbered traffic district with higher crowd gathering are: NO. 3,7,23,38,68,77,82,103,110. The common feature of these neighborhoods is that they are all commercial land gathering places as well as residential land. In these neighborhoods, there is a higher population flow and they are higher crowd gathering type, so these districts can be the focus of urban planning and management optimization.

Fig. 10 shows the changes in the relative active population equivalents of 111 different numbered traffic districts for a total of 90 moments per day. The horizontal axis represents the numbered traffic districts

and the vertical axis represents 90 moments, with three statistical moments as one unit, and the color squares represent the difference in the relative active

population equivalents of the same numbered district at adjacent moments.

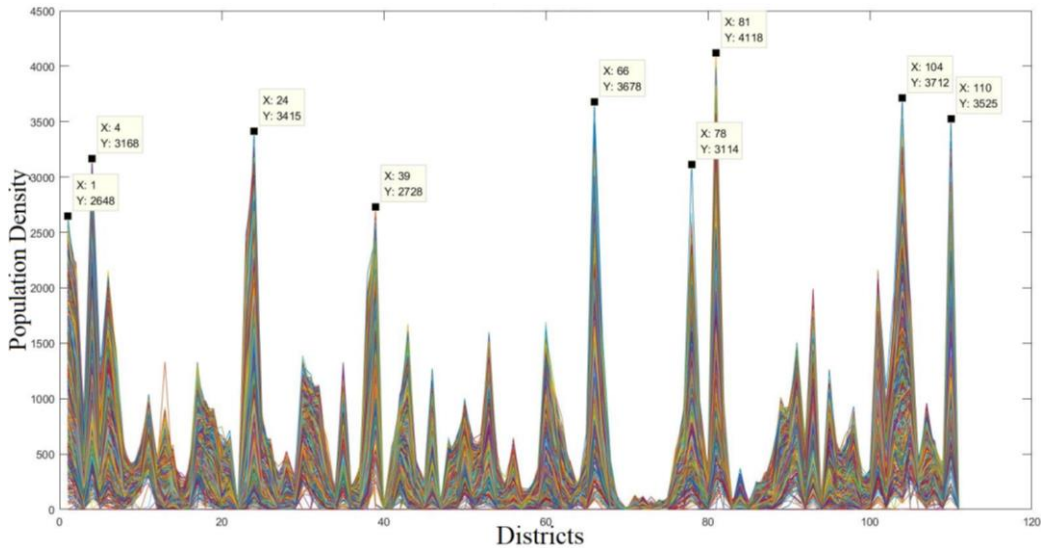


Fig. 9. Crowd gathering of each traffic district

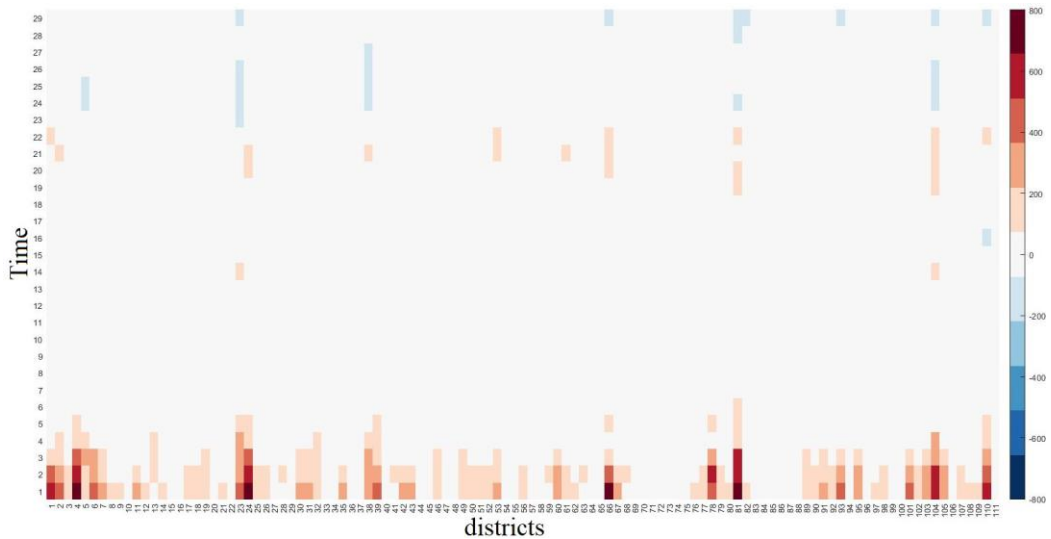


Fig. 10. Change in relative active population in traffic districts

From Fig. 10, it can be seen that the number of active population equivalents in the same numbered traffic district increases significantly during the day from 7:03 a.m. to 9:03 a.m. From 16:33 p.m. to 18:03 p.m., there is a small increase in the number of active population equivalents in each numbered traffic district, and from 18:33 p.m. to 21:53 p.m., the number of active population equivalents gradually decreases. The numbered districts with larger changes in crowd gathering during the day are: NO. 4, 24, 66, 81, 104, 110. At the same time, the numbered districts with a more significant increase in the number of active population during the time period from 7:03 a.m. to 9:03 a.m. are: NO. 22, 38, 66, 81, 104, 110, as shown in Fig. 11. These traffic districts have an unbalanced change in the number of active population during the day, which is highly likely to cause traffic congestion.

6. Conclusions

In this paper, the Baidu Heatmap of Chongqing urban core area is used to identify and extract different colors in the map. It uses the relationship between the density of people and different traffic districts in the city to build a mathematical model, and solve the relative active population density equivalent corresponding to different color categories. Using the parameter of population intensity, it studies the spatial

and temporal distribution characteristics of residents' travel activities in the urban core area of the city.

Through data processing and analysis, it can be concluded that in the core area, the crowd gathering mainly has the following characteristics.

(1) In a day, the gathering degree of the crowd has the maximum and minimum, and the corresponding time is 18:33 and 07:03 respectively. From 07:03 to 09:33 in the morning, the degree of crowd gathering is significantly enhanced.

(2) Compared with the rest day, the significant change of crowd gathering degree on the working day is one hour earlier, and the peak of crowd gathering on the rest day is around 12:03 p.m. The relative active population equivalent in the afternoon of the working day is greater than the corresponding value in the morning, while the relative active population equivalent in the noon of the rest day is greater than the corresponding value in any other period of the day.

(3) It is found that the crowd gathering degree of 9 traffic districts changes more significantly every day, which indicates that these districts have a larger population mobility and greater traffic pressure compared with other districts. In urban traffic planning and treatment, these traffic districts should be taken as the object of key optimization management.

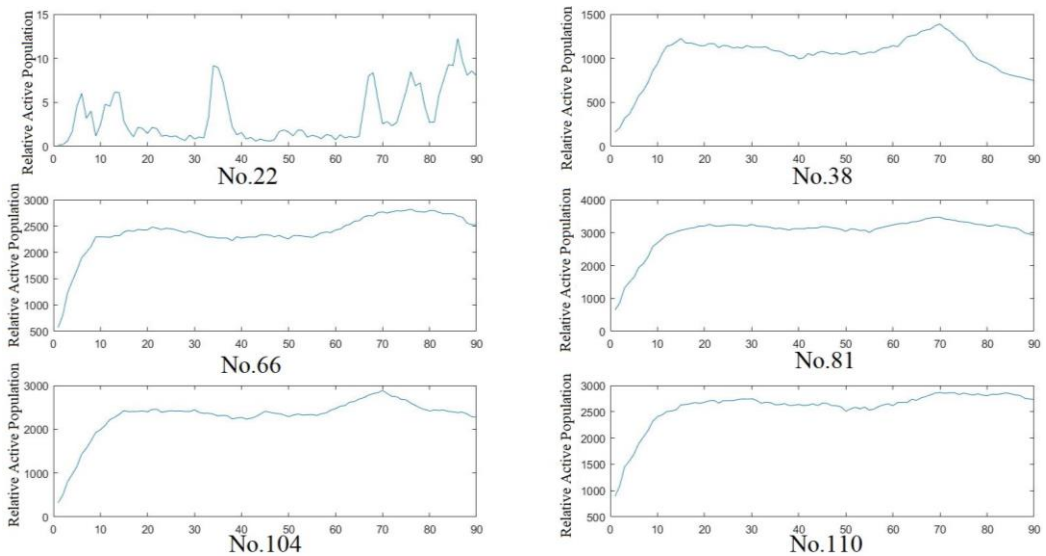


Fig. 11. Districts with significant changes in population numbers

Acknowledgements

This research was supported by the Graduate Research Innovation Project of Chongqing Jiaotong University (No CYS22408), Graduate Joint Training Base Construction Project of Chongqing (No. JDLHPYJD- 2020029).

References

- [1] Bao, C., Zhang, S. (2018). Route Optimization of cold chain logistics in joint distribution with consideration of carbon emission. *Industrial Engineering and Management*, 23(05): 95-100+107. <https://doi.org/10.19495/j.cnki.1007-5429.2018.05.013>.
- [2] Bao, X., Song, A. (2023). Improved NSGA-II algorithm for solving multi-objective logistics vehicle routing optimization problem. *Computer Applications and Software*, 40(02): 274-280. <https://doi.org/10.3969/j.issn.1000-386x.2023.02.043>.
- [3] Büşra, O., Çağrı, K., Fulya, A. (2021). A Hyper Heuristic for the Green vehicle routing problem with simultaneous pickup and Delivery. *Computers & Industrial Engineering*, 153. <https://doi.org/10.1016/j.cie.2020.107010>.
- [4] Elhedhli, S., Merrick, R. (2012). Green supply chain network design to reduce carbon emissions. *Transportation Research Part D*, 17(5): 370-379. <https://doi.org/10.1016/j.trd.2012.02.002>.
- [5] Gao, Y. (2006). Non-dominated sorting genetic algorithm and its applications. Zhejiang University.
- [6] Guo, X., Zhang, W., Liu, B. (2022). Low-carbon routing for cold-chain logistics considering the time-dependent effects of traffic congestion. *Transportation Research Part D*, 113. <https://doi.org/10.1016/j.trd.2022.103502>.
- [7] He, D., Li, Y. (2018). Optimization model of green multi-type vehicles routing problem. *Journal of Computer Applications*, 38(12): 3618-3624+3637. <https://doi.org/10.11772/j.issn.1001-9081.2018051085>.
- [8] Ji, Y., Du, J., Wu, X. (2021). Robust optimization approach to two-echelon agricultural cold chain logistics considering carbon emission and stochastic demand. *Environment, Development and Sustainability*, 23, 13731-13754. <https://doi.org/10.1007/s10668-021-01236-z>.
- [9] Leng, L. (2020). Research on low-carbon logistics location-routing problem and hyper-heuristic algorithm. Zhejiang University of Technology. <https://doi.org/10.27463/d.cnki.gzgyu.2020.000009>.
- [10] Li, B., Zhao, G. (2017). Model of low-carbon remanufacturing logistics network based on robust optimization. *Journal of Shandong University (Science Edition)*, 52(01): 43-55. <https://doi.org/10.6040/j.issn.1671-9352.0.2016.174>.
- [11] Li, C., Li, S., Liu, S. (2020). Research on urban logistics distribution network from the perspective of low-carbon. *Ecological Economics*, 36(01): 106-110.
- [12] Li, J. (2015). Credibility-based Multi-objective fuzzy programming problem for low-carbon logistics network design. *Systems Engineering-Theory & Practice*, 35(06): 1482-1492.
- [13] Li, Q. (2022). Research on multi-objective agricultural cold chain logistics vehicle path planning. Tianjin Normal University. <https://doi.org/10.27363/d.cnki.gtsfu.2022.000365>.
- [14] Li, W., Zhang, C., Ma, C. (2020). An optimization model and solution algorithm of Multi-objective vehicle path under low carbon conditions. *Traffic Information and Safety*, 38(01): 118-126+144. <https://doi.org/10.3963/j.jssn.1674-4861.2020.01.015>.
- [15] Liu, F. (2022). Research on logistics distribution fleet configuration and route optimization under low carbon. Shandong University. <https://doi.org/10.27272/d.cnki.gshdu.2022.005427>.
- [16] Liu, S., Zhang, C. (2023). Multiobjective optimization of railway cold-chain transportation route based on dynamic train information. *Journal of Rail Transport Planning & Management*, 26. <https://doi.org/10.1016/j.jrtpm.2023.100381>.
- [17] Lv, P. (2013). Study of logistics network optimization model considering carbon emission. *Application Research of Computer*, 30(10): 2977-2980. <https://doi.org/10.3969/j.issn.1001-3695.2013.10.024>.

- [18] Martinez-Puras, A., Pacheco, J. (2016). MO-AMP-Tabu search and NSGA-II for a real bi-objective scheduling-routing problem. *Knowledge-Based Systems*, (112): 92-104. <https://doi.org/10.1016/j.knosys.2016.09.001>.
- [19] Masoud, H., Mohammad Ali, F., Ali, H. (2023). A two-echelon location routing problem considering sustainability and hybrid open and closed routes under uncertainty. *Heliyon*, 9(3). <https://doi.org/10.1016/j.heliyon.2023.e14258>.
- [20] Peng, Y., Mo, Z., Liu, S. (2021). Passenger's routes planning in stochastic common-lines' multi-modal transportation network through integrating Genetic Algorithm and Monte Carlo simulation. *Archives of Transport*, 59(3), 73-92. <https://doi.org/10.5604/01.3001.0015.0123>.
- [21] Ren, T., Luo, T., Gu, Z. (2022). Optimization of urban logistics co-distribution path considering simultaneous pick-up and delivery. *Computer Integrated Manufacturing System*, 28(11): 3523-3534. <https://doi.org/10.13196/j.cims.2022.11.016>.
- [22] Song, M., Li, J., Han, Y. (2020). Metaheuristics for solving the vehicle routing problem with the time windows and energy consumption in cold chain logistics. *Applied Soft Computing Journal*, 95: 106561. <https://doi.org/10.1016/j.asoc.2020.106561>.
- [23] Tong, H., (2022). Research on the site selection and path layout of the logistics distribution center of marine ships based on a mathematical model. *Archives of Transport*, 63(3), 23-34. <https://doi.org/10.5604/01.3001.0015.9925>.
- [24] Vincent, F.Y., Pham, T., Roberto, B. (2023). A robust optimization approach for the vehicle routing problem with cross-docking under demand uncertainty. *Transportation Research Part E*, 173. <https://doi.org/10.1016/j.tre.2023.103106>.
- [25] Wang, Y., Shi, Q., Song, W. (2020). Dynamic multi-objective optimization model and algorithm for logistics networks. *Computer Integrated Manufacturing Systems*, 26(04): 1142-1150. <https://doi.org/10.13196/j.cims.2020.04.027>.
- [26] Yang, J., Guo, J., Ma, S. (2016). Low-carbon city logistics distribution network design with resource deployment. *Journal of Cleaner Production*, 2016, 119: 223-228. <https://doi.org/10.1016/j.jclepro.2013.11.011>.
- [27] Yuan, Y., Diego, C., Maxime, O., (2021). A column generation based heuristic for the generalized vehicle routing problem with time windows. *Transportation Research Part E*, 152. <https://doi.org/10.1016/j.tre.2021.102391>.
- [28] Zhang, D., Qiao, X., Xiao, B., (2021). Multi-objective vehicle routing optimization based on low carbon perspective and random demand. *Journal of Railway Science and Engineering*, 18(08): 2165-2174. <https://doi.org/10.19713/j.cnki.43-1423/u.T20200883>.
- [29] Zhang, L., Tseng, M., Wang, C., (2019) Low-carbon cold chain logistics using ribonucleic acid-ant colony optimization algorithm. *Journal of Cleaner Production*, 233: 169-180. <https://doi.org/10.1016/j.jclepro.2019.05.306>.
- [30] Zhang, S., Chen, N., Li, Y. (2022). Research on optimization decision of urban cold chain logistics distribution system from perspective of low carbon. *Industrial Engineering and Management*, 27(01): 56-64. <https://doi.org/10.19495/j.cnki.1007-5429.2022.01.007>.
- [31] Zhu, A., Wen, Y. (2021). Green logistics location-routing optimization solution based on improved GA Algorithm considering low-carbon and environmental protection. *Journal of Mathematics*. <https://doi.org/10.1155/2021/6101194>.